SLAC-PUB-16468

Revealing W51C as a Cosmic-Ray source using *Fermi*-LAT data

T. Jogler[1,2] and S. Funk[1,2]

Received ______________________; accepted ______________________

[1]W. W. Hansen Experimental Physics Laboratory, Kavli Institute for Particle Astrophysics and Cosmology, Department of Physics and SLAC National Accelerator Laboratory, Stanford University, Stanford, CA 94305, USA

[2]Erlangen Centre for Astroparticle Physics, D-91058 Erlangen, Germany

[3]email: jogler@slac.stanford.edu

This material is based upon work supported by the U.S. Department of Energy, Office of Science, Office of Basic Energy Sciences, under Contract No. DE-AC02-76SF00515.

ABSTRACT

Supernova remnants (SNRs) are commonly believed to be the primary sources of Galactic cosmic rays. Despite the intensive study of the non-thermal emission of many SNRs the identification of the accelerated particle type relies heavily on assumptions of ambient medium parameters that are only loosely constrained. Compelling evidence of hadronic acceleration can be provided by detecting a strong roll-off in the secondary γ rays spectrum below the π^0 production threshold energy of about 135 MeV, the so called "pion bump". Here we use five years of *Fermi*-LAT data to study the spectrum above 60 MeV of the middle-aged SNR W51C. A clear break in the power-law γ-ray spectrum at $E_{\text{break}} = 290 \pm 20$ MeV is detected with $9\,\sigma$ significance and we show that this break is most likely associated with the energy production threshold of π^0 mesons. A high-energy break in the γ-ray spectrum at about 2.7 GeV is found with $7.5\,\sigma$ significance. The spectral index at energies beyond this second break is $\Gamma_2 = 2.52^{+0.06}_{-0.07}$ and closely matches with the spectral index derived by the MAGIC Collaboration above 75 GeV. Therefore our analysis provides strong evidence to explain the γ-ray spectrum of W51C by a single particle population of protons with a momentum spectrum best described by a broken power-law with break momentum $p_{\text{break}} \sim 80$ GeV c^{-1}. W51C is the third middle-aged SNR that displays compelling evidence for cosmic-ray acceleration and thus strengthens the case of SNRs as the main source of Galactic cosmic rays.

Subject headings: gamma rays: general — γ rays— SNRs – observation: individual (W51C)

1. Introduction

Supernova remnants (SNRs) are widely believed to be the sources of Galactic cosmic rays ($E < 10^{15}$ eV). The verification of this hypothesis is possible by studying the γ-ray emission from SNRs. The accelerated cosmic rays interact with surrounding matter and produce π^0 mesons that sub-sequentially decay into γ rays leading to a characteristic break in the γ-ray spectrum at about $E \sim$ 200–300 MeV due to the finite rest mass of the π^0. Competing leptonic γ-ray production mechanisms such as bremsstrahlung and inverse Compton (IC) emission require strong fine tuning to produce a similar feature.[1] The pion bump is thus an unmistakable feature of hadronic origin of γ-ray emission that is observable by the *Fermi*-Large Area Telescope (LAT). This feature was recently found in the two brightest *Fermi*-LAT detected SNRs, IC 443 and W44 as reported in Ackermann et al. (2013). The third brightest *Fermi*-LAT detected SNR W51C is another prime candidate to search for the pion-decay signature in the γ-ray emission because it is interacting with a molecular cloud (MC) that poses an excellent target for cosmic-ray interactions and subsequent π^0-decay.

W51C is an SNR identified by its radio shell and assumed to be 30 kyr old and at a distance of 5.5 kpc (Sato et al. 2010). The SNR belongs to the larger W51 complex composed of one of the largest star-forming regions in our Galaxy divided into two parts denoted W51A and W51B. The SNR is located towards the south-eastern end of W51B and evidence for interaction between the SNR shell and the W51B MC is provided by the discovery of two OH (1720 MHz) masers by Green et al. (1997). Further evidence is provided by high-velocity atomic gas that shows velocity shifts between 20 km s^{-1} and 120 km s^{-1} with respect to the ambient medium (Koo and Moon 1997). The OH masers and the high-velocity clouds are commonly interpreted as

[1]The break required in the right position of the lepton energy spectrum and the extremely hard spectral index, unexplainable by conventional diffuse shock acceleration, render leptonic model explanations unlikely.

the result of shock waves penetrating into MCs. More recent measurements by Ceccarelli et al. (2011) find an over-abundance of over-ionized gas in certain W51B locations close to W51C that they interpret as the result of ionization through by-products of freshly accelerated cosmic rays interacting with nucleons. All these measurements outline a compelling scenario in which the W51C SNR shell is interacting with the MC W51B.

X-ray imaging of the region revealed a hard source denoted CXO J192318.5+140305, that was identified as a possible pulsar wind nebula (PWN) related to the SNR (Koo et al. 2002, 2005). Such a PWN could also power relativistic particle acceleration resulting in γ-ray emission.

W51C was detected in 11 month of data by the *Fermi*-LAT and showed spatially extended γ-ray emission above $E > 2$ GeV. The γ-ray spectrum showed curvature that required a break at a few GeV and subsequent modeling by a hadronic spectrum required a broken power-law for the proton spectrum with a break momentum of $10 - 15$ GeV c^{-1} (Abdo et al. 2009). At very high energies ($E > 100$ GeV, VHE) an energy-dependent morphology was revealed by the MAGIC collaboration (Aleksić et al. 2012). No hint of spectral variation could be identified and the emission is attributed to the SNR W51C due to its morphology and multi-wavelength modeling of the spectral energy distribution (SED). The authors mention that a contribution of up to 20% of the W51C flux could come from the PWN candidate CXO J192318.5+140305. A final determination of the parent particle population that creates the γ rays was not possible, though multi-wavelength interpretation of the SED of W51C favors a hadronic origin of the γ-ray emission.

Here we analyze five years of *Fermi*-LAT data and search for features that can identify the parent particle type in the most detailed γ-ray spectrum of W51C derived to date.

2. Observations & Data Analysis

The Large Area Telescope (LAT), the primary instrument of the *Fermi Gamma-ray Space Telescope* mission, is a pair-conversion telescope sensitive to γ rays in an energy range from 20 MeV to $E > 300$ GeV. For a more detailed description the reader is referred to Atwood et al. (2009) and for the on-orbit performance to Ackermann et al. (2012). We analyzed public *Fermi*-LAT data between MJD 54682.7 and MJD 56516.5 corresponding to about five years of Pass 7 Reprocessed data. The data are analyzed using the `Fermi ScienceTools` version v9r32p04[2]. We select events with high probability of being γ rays by choosing the SOURCE event class. In order to evade γ-ray contamination generated by cosmic rays hitting the Earth's atmosphere, we remove time intervals when the field of view of the LAT came too close to the Earth limb (zenith angle$< 100°$). We analyze data between 60 MeV and 300 GeV and use the P7REP_SOURCE_V15 instrument response functions (IRFs). To account for the interstellar γ-ray emission caused by cosmic rays interacting with gas or interstellar radidation in our Galaxy, the gll_iem_v05_rev1.fit model is used. This interstellar emission model (IEM) is our standard IEM provided by the *Fermi*-LAT collaboration for point source analysis. The isotropic γ-ray emission is accounted for by the iso_source_v05.txt model that also includes any residual charged particle background present in the *Fermi*-LAT data. We chose a $20° \times 20°$ region of interest (ROI) centered on W51C and performed a binned likelihood analysis with $0\overset{\circ}{.}1$ bins and 30 logarithmically spaced bins in energy.

We construct a test statistic (TS) following Mattox et al. (1996) to evaluate the improvement of the likelihood fit to the ROI when adding a new source. In the case of one additional source with one additional free parameter we can define $TS = 2(L - L_0)$ and the significance as $\sigma = \sqrt{TS}$

---

[2]Both the data as well as the associated software packages along with the templates used to model the interstellar and extragalactic emission are publicly made available by the *Fermi* Science Support Center http://fermi.gsfc.nasa.gov/ssc/data/.

where L_0 and L are the log-likelihood values without the source and with it respectively.

In order to study the effect of nearby sources on the spectral fit of W51C we use `gtobssim`[3] to obtain Monte Carlo simulations of the W51C region. In our simulations we assume spectral values for all sources as given in the 3FGL catalog (Acero et al. 2015). We vary all independent spectral parameters randomly by either $+2\sigma$ or -2σ of the associated error. The $\pm 2\sigma$ is chosen to provide an estimation in the case of a strong deviation of the real spectral value compared to the 3FGL catalog and at the same time to require running only a few simulations. We run ten variations of the simulation so that different combinations of sources have positive and negative fluctuations. Afterwards we analyze these ten Monte Carlo simulation samples with varying free parameters for the likelihood fit of the background sources. Finally, we compare the fit results of W51C with the simulated values for each analysis. We find that we only have to leave parameters of the five sources marked with cyan crosses in Fig. 1 free in the likelihoodfit to obtain within statistical uncertainties the simulated parameter values of W51C. For sources with $TS < 50$ in the 3FGL catalog we leave only the normalization free and for more significant sources all other independent spectral parameters too. In addition to the sources in Fig. 1 we also leave the normalizations of the IEM and the isotropic emission template free in our analysis.

To estimate the systematic uncertainties on flux and spectral properties of W51C caused by our limited knowledge of the IEM we compare the standard IEM results to the results obtained with eight alternative models generated with GALPROP (Vladimirov et al. 2011) and afterwards refined by fitting to the *Fermi*-LAT data. Each of these models consists of eight map cubes (i.e., three dimensional models of gamma-ray intensity as a function of position and energy) inferring the interstellar γ-ray emission from gas by tracing it with H I and CO maps. The H I and CO maps are divided into the contribution from four galactocentric rings. In addition to these contributions there are map cubes added for large residual structures in the *Fermi*-LAT γ-ray sky, namely

[3]For further information see http://fermi.gsfc.nasa.gov/ssc/data/analysis/scitools/obssim_tutorial.html

Loop I (Casandjian et al. 2009), the *Fermi* bubbles (Su et al. 2010; Ackermann et al. 2014) and an inverse Compton (IC) emission map. For a more detailed explanation of the alternative models see Ackermann et al. (2015). Inside the W51C ROI only the H I rings 2–4, the CO rings 2–4, the IC map and the Loop I template give any background contribution and all other components are removed from our fits. In addition to these components an IEM-specific isotropic component is added.

In our IEM systematic uncertainty study the normalizations of the individual components of each IEM are free in the likelihood fit. The alternative IEMs provide more freedom to the fit by leaving the components individually adjustable instead of only one global normalization as in the case of the standard IEM.

3. The W51C region as seen by *Fermi*-LAT

W51C was already reported to be an extended source for the *Fermi*-LAT in Abdo et al. (2009). We use the `pointlike` code (Kerr 2011) to verify whether our data set, which is more than five times larger than that used in Abdo et al. (2009) would allow us to further constrain the morphology of W51C. Therefore we divide the γ-ray emission into energy bands from 60 MeV to 1 GeV, 1–5 GeV and 5–300 GeV. The energy ranges are chosen to separate the individual spectral regimes present in the W51C γ-ray spectrum (see Sec. 4) and simultaneously include high photon statistics in each bin. No solid evidence for changing morphology between the tested energy bands is found. Slight differences in the position, geometry and shape of the γ-ray excess that are seen between the individual energy bands have no impact on the obtained photon spectrum and thus are negligible for the spectral analysis of W51C. In our study W51C is modeled by a flat elliptical disk with five free parameters (R.A., Dec., minor axis, major axis, rotation angle). In the best-position fit we use the best-fit spectral values obtained with the previously published

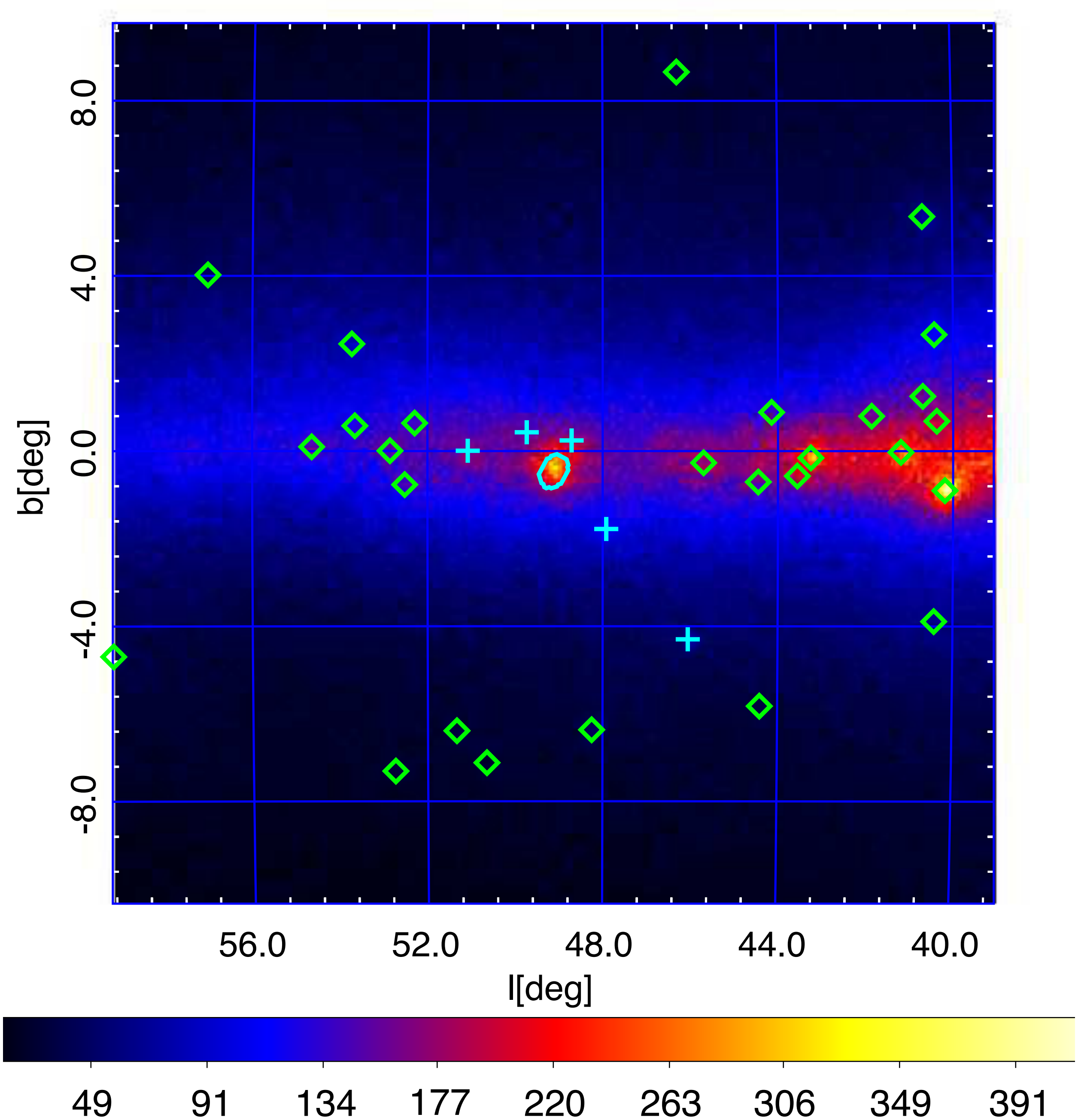

Fig. 1.— Photon counts map above 60 MeV for the five years of *Fermi*-LAT data. Sources with spectral parameters left free in the likelihood-fit are shown as cyan crosses and all other sources as green diamonds. The W51C template contour is the cyan ellipse in the center. W51C is the brightest source in the central region of the ROI.

template[4] and afterwards verify that leaving the spectral parameters free in the position fit does not alter the spatial shape or position. A fit using a two-dimensional Gaussian instead of the elliptical disk does not result in an improvement of the overall description of the region and has only insignificant effects on the W51C fit results. Our best-fit morphology for the overall energy range is in good agreement with the previously published template of W51C and we use this publicly available template for all our studies.

Comparing the morphology of W51C seen by the *Fermi*-LAT with the one obtained by MAGIC shows a spatial coincidence as seen in Fig. 2. The MAGIC contours are not an exact match to the *Fermi*-LAT template but they completely overlap. The difference between the two shapes might be explained by the lower angular resolution of the *Fermi*-LAT making it impossible as shown in Lande et al. (2012) to distinguish between very similar source shapes. We conclude from these comparisons that the energy-dependent morphology changes seen by MAGIC cannot be detected at $E < 75$ GeV by *Fermi*-LAT .

4. Search for the Pion cut-off in W51C

We fit the W51C flux in 20 logarithmic energy bins independently between 60 MeV and 300 GeV. The resulting SED is shown in Fig. 3 and a clear low-energy break around 300 MeV is visible. The SEDs obtained using the alternative IEMs differs by more than the statistical errors only at energies below a few GeV. All of them indicate a low-energy break at a very similar energy as the standard IEM. Above about 1 GeV there are only very small differences between the SEDs derived with the alternative IEMs and the standard one, as expected since the diffuse emission from cosmic-ray interactions decreases more rapidly than the source spectrum.

The significance of the break is obtained by fitting W51C using the likelihood approach

[4]Available from: http://fermi.gsfc.nasa.gov/ssc/data/analysis/LAT_essentials.html

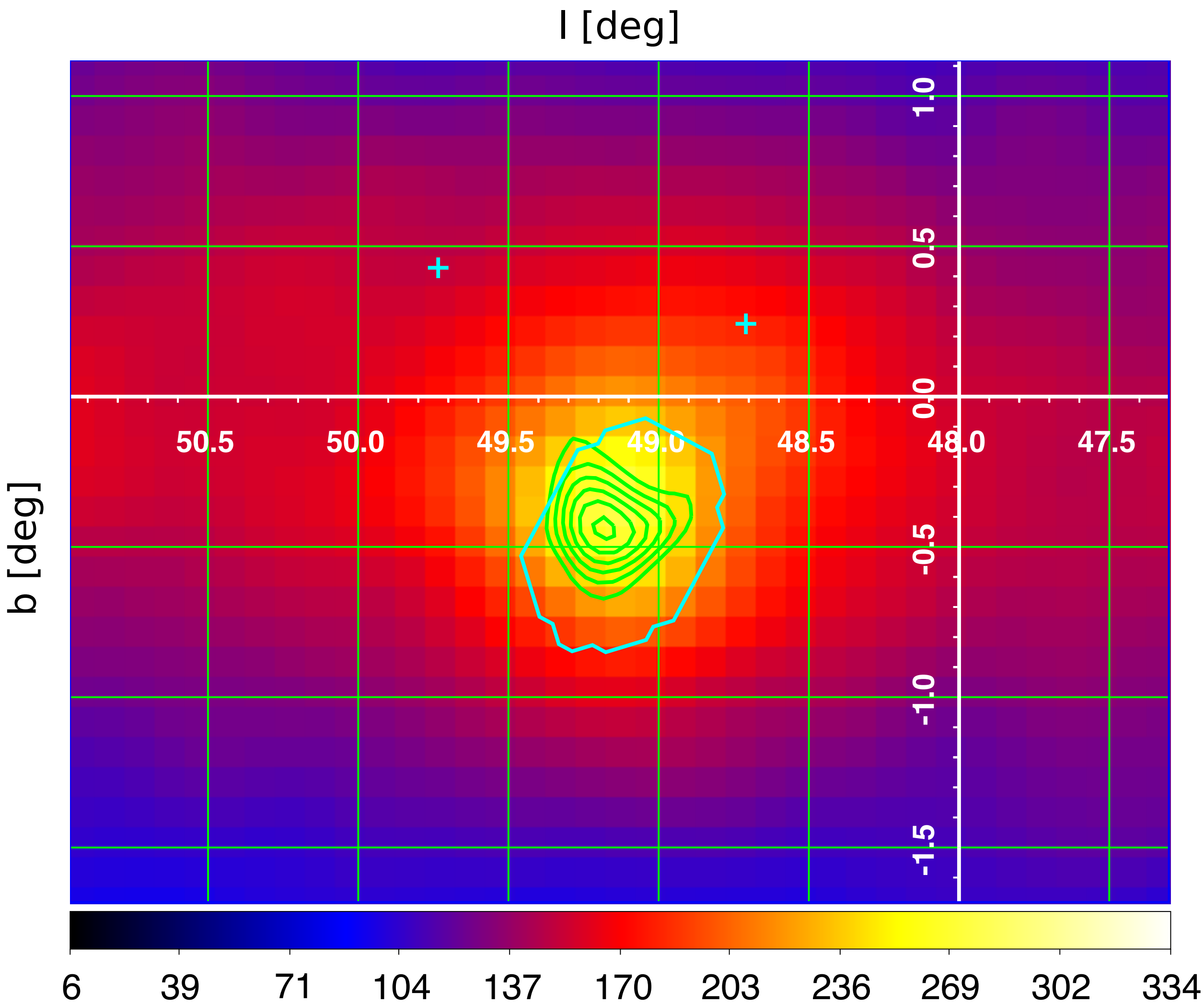

Fig. 2.— The *Fermi*-LAT photon counts map of W51C above 60 MeV is shown in color scale; overlaid are the *Fermi*-LAT W51C template in a cyan contour and the MAGIC W51C significance contours (Aleksić et al. 2012) above 150 GeV in green. Nearby *Fermi*-LAT sources from the 3FGL catalog are marked by crosses. The overlap of both contours suggests that MAGIC and *Fermi*-LAT detect emission from the same region while the broader PSF of *Fermi*-LAT at low energies makes more detailed comparisons impossible.

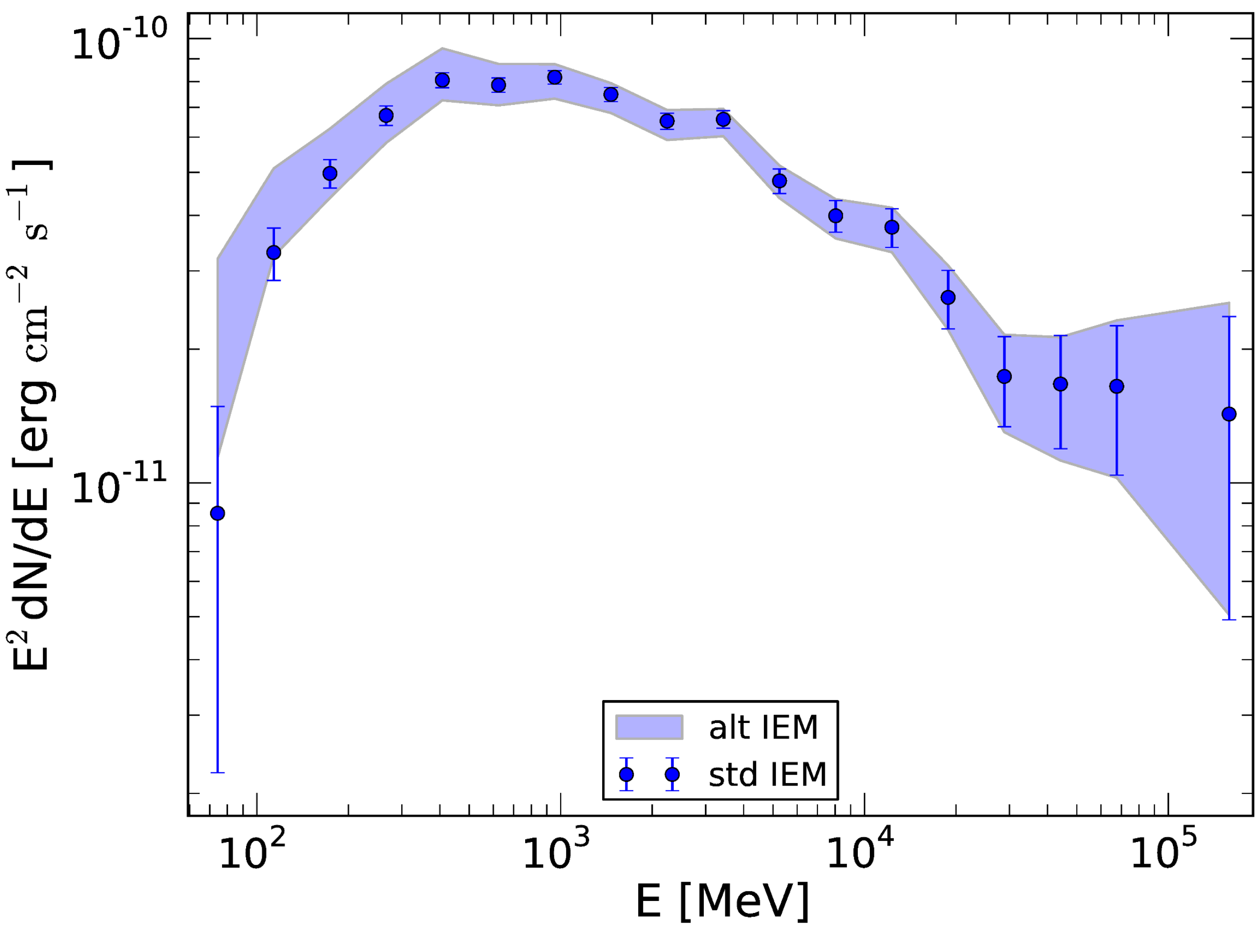

Fig. 3.— The W51C SED as obtained from the *Fermi*-LAT data using the standard IEM (points). The envelope over all statistical error bars of the eight alternative IEM SEDs is shown by the blue band. A break in the SED around 300 MeV, as well as a second one at about 3 GeV, are clearly visible for all the IEMs used.

between 60 MeV and 3 GeV once with a smoothly broken power law of the form $F(E) = N_0(E/E_0)^{\Gamma_1}[1 + (E/E_{\rm break})^{(\Gamma_1-\Gamma_2)/\alpha}]^{-\alpha}$, with E_0= 200 MeV and $\alpha = 0.1$ and once with a power law of the form $F(E) = N_0(E/E_0)^{-\Gamma}$. The improvement in likelihood when fitting a smoothly broken power law and assuming a nested model with two additional degrees of freedom yields a 9σ significance for a spectral break at $E_{\rm break} = 290 \pm 20$ MeV and change of spectral index from $\Gamma_1 = 0.70^{+0.23}_{-0.28}$ to $\Gamma_2 = 2.15 \pm 0.03$. To estimate the systematic uncertainty of the break energy due to our limited knowledge of the *Fermi*-LAT IRFs the bracketing IRFs method is used (Ackermann et al. 2012). Here the worst-case scenario, in which the IRFs change maximally at the break energy, is assumed to provide conservative systematic uncertainties. Additionally we apply the same method using the eight alternative IEMs and obtain very similar results for $E_{\rm break}$. The alternative IEM fits allow us to estimate the systemaitc uncertainty of the break energy by calculating the variance with respect to the standard IEM (Ackermann et al. 2015). Furthermore, the smoothly broken power law is favored above a power law in all alternative models and yields at least a significance of $8.7\,\sigma$ rendering the break significant in all IEMs tested. The variation of the IEMs is our currently best method to estimate uncertainties associated to our limited knowledge of the IEM but can not provide a complete coverage of all possible deviations. Taking into account the aforementioned uncertainties we obtain a clear low-energy break in the W51C spectrum at $E_{\rm break} = 290 \pm 20({\rm stat}) \pm 40({\rm syst, IEM}) \pm 30({\rm syst, IRF})$ MeV. In addition we also test for the effect of energy dispersion that results in general in an over prediction of the lowest flux point in the SED by about 30%. Similar to the study in Ackermann et al. (2013) we find that neglecting energy dispersion in our analysis leads to a lower significance of the detected low-energy break. The break in W51C shows very similar properties ($E_{\rm break}$, Γ_1, Γ_2) compared to those of the SNRs W44 and IC 443 that were already identified convincingly cosmic-ray accelerators (Ackermann et al. 2013).

Closer inspection of the W51C SED suggests that there is also a high-energy break in the spectrum. Indeed such a break is expected since the spectral index above the low-energy break

$\Gamma_2 = 2.15 \pm 0.03$ is not compatible with the one obtained by the MAGIC collaboration at energies beyond 75 GeV of $\Gamma = 2.58 \pm 0.07$ (Aleksić et al. 2012). Applying the same likelihood approach as for the low-energy break but using the energy range 400 MeV to 300 GeV to compare between smooth-broken power-law and simple power-law we find a break at $E_{\text{break,HE}} = 2.7^{+1.0}_{-0.8}(\text{stat})$ GeV with $7.5\,\sigma$ significance. Systematic uncertainties due to the IEM are unimportant at these energies and given the large statistical uncertainty all systematic errors are negligible in comparison. The power-law spectral index changes from $\Gamma_1 = 2.11^{+0.06}_{-0.05}$ in the low-energy regime to $\Gamma_2 = 2.52^{+0.06}_{-0.07}$ above the break. The high-energy spectral index is in excellent agreement with the spectral index reported by the MAGIC collaboration at energies above 75 GeV and thus the MAGIC spectrum can be well explained by the same particle population as the Fermi emission above $E_{\text{break,HE}}$. In the next section the origin of the γ-ray emission is tested with hadronic and leptonic scenarios.

5. Modeling the W51C SED

The obtained W51C SED is fitted by a proton-induced and alternatively by an electron-induced γ-ray spectrum. For the case of the electron-induced spectrum we consider IC and bremsstrahlung dominated γ-ray production. The γ-ray spectra for the leptonic cases are calculated according to the cross sections given in Blumenthal and Gould (1970) and Baring et al. (1999) for the electron-electron bremsstrahlungs cross-section. The IC seed photons are provided by the cosmic microwave background (CMB), the emission of infrared light, mainly from dust, and star light. Each of these seed photon fields is modeled by a black body spectrum with $kT_{\text{CMB}} = 2.3 \times 10^{-4}$ eV, $u_{\text{CMB}} = 0.26$ eV cm^{-3} for the CMB, $kT_{\text{IR}} = 3 \times 10^{-3}$ eV, $u_{\text{IR}} = 0.90$ eV cm^{-3} for the infrared light and $kT_{\text{Star}} = 0.25$ eV, $u_{\text{Star}} = 0.84$ eV cm^{-3} for the star light. The values are taken from Abdo et al. (2009). We also consider cooling effects due to synchrotron emission for electrons above 1 TeV for which we assume a constant injection. Other cooling channels are unimportant for the assumed acceleration lifetime of the SNR (30 kyr) and thus neglected. The proton-proton cross sections are taken from Kamae et al. (2006) and we multiply them by a factor of 1.85 to account for heavier element abundance as suggested by Mori (2009). Secondary spectra from the decay of charged pions are computed as well but found to contribute insignificantly to the total γ-ray emission and hence are neglected.

For all tested processes the parent particle spectrum is modeled by a broken power law with an exponential cut-off in momentum space. A comparison with a simple power law with exponential cut-off yields much worse results for bremsstrahlung and IC processes and a slightly worse description in the case of the hadronic spectrum. We note that we only use statistical errors when fitting the SED.

The best-fit spectra are shown in Fig. 4 and the only adequate description of the *Fermi*-LAT data is provided by the proton induced emission spectrum. Including the MAGIC data in the fit yields again only a valid description with the proton spectrum with a $(\chi^2/d.o.f.)_{\rm pp} = 26.3/22$, whereas the χ^2 values of the IC $(\chi^2/d.o.f.)_{\rm IC} = 484/23$ and bremsstrahlungs spectra $(\chi^2/d.o.f.)_{\rm Brems} = 98.5/23$ indicate an insufficient description of the data. More complicated spectral shapes that allow for another low-energy break in the lepton spectrum might be able to explain the W51C spectrum as due to bremsstrahlungs processes but again that would require strong fine tuning. Therefore we find the hadronic explanation of the γ-ray spectrum the most convincing model.

We also fitted the SEDs obtained using the alternative IEMs to asses the modeling dependency to the dominant systematic uncertainties with the aforementioned processes. The proton-proton mechanism is always significantly favored above the bremsstrahlungs description.

The proton spectrum has a rather soft spectral index below the break of $\Gamma_1 = 2.48 \pm 0.02$ compared to the $\Gamma = 2.0$ or harder predicted by DSA. However, we note that fixing the spectral index to $\Gamma = 2.0$ results in a worse but perhaps still acceptable $\chi^2/d.o.f. = 47.8/23$ value. Also the two other SNRs IC 443 and W44 that are identified proton accelerators show rather soft

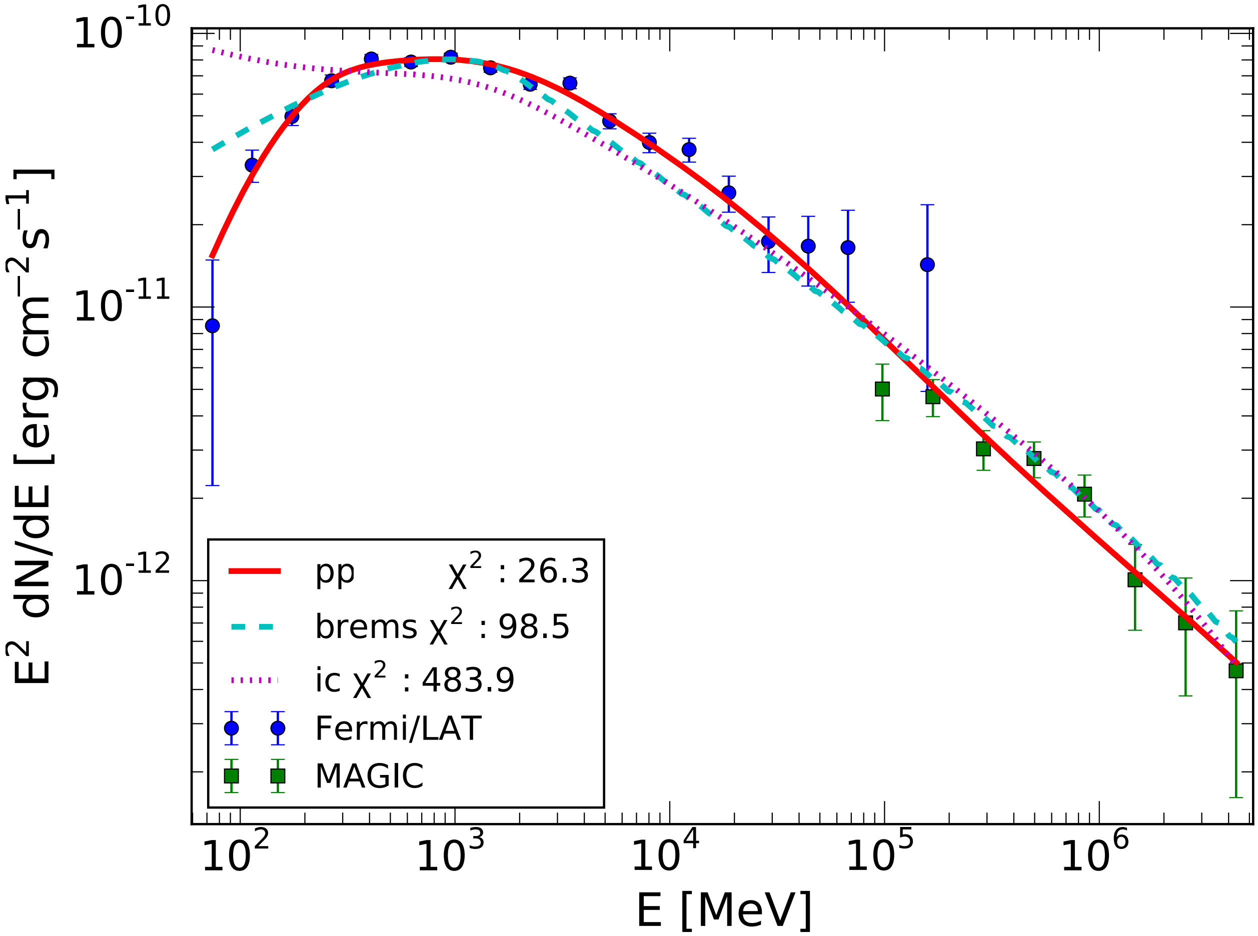

Fig. 4.— (color online) The W51C SED as obtained from the *Fermi* data (blue points) and MAGIC data (green squares). The best-fit models for pp interaction (solid red), bremsstrahlung (dashed cyan) and IC (dotted magenta) induced γ-ray emission are shown together with their χ^2 values. Only the proton-proton model describes the data reasonably.

spectral indices ($\Gamma = 2.36$) very similar to W51C.

We determine the break momentum to $p_{\text{break}} = 81.3^{+5.8}_{-5.4}\,\text{GeV}/c$ and the high-energy spectral index to $\Gamma_2 = 2.73 \pm 0.03$. Our fit does not allow for a determination of the exponential cut-off, we find by profiling the cut-off momentum that any value between $p_{\text{cut}} = 30\,\text{TeV}$ and $p_{\text{cut}} = 300\,\text{TeV}$ yields a $\Delta\chi^2 < 3.7$.

6. Conclusion

We establish a low-energy break at $E_{\text{break}} = 290 \pm -20(\text{stat}) \pm 40_{\text{syst,IEM}} \pm 30_{\text{syst,IRF}}$ MeV in the γ-ray spectrum of W51C. This break is associated with the energy threshold of π^0 production and hence a strong evidence of the hadronic origin of the γ-ray emission. Furthermore, we establish a second break in the photon spectrum at $E_{\text{break,HE}} = 2.7^{1.0}_{-0.8}(\text{stat})$ GeV that smoothly connects the *Fermi*-LAT spectrum and the spectrum obtained by the MAGIC collaboration above 75 GeV. The best description of the combined *Fermi*-LAT and MAGIC SED is given by a proton-proton induced γ-ray spectrum with a broken- power-law spectrum in momentum space of the parent particles.

These results make W51C the third undoubtedly identified cosmic-ray accelerating SNR. As with the other two SNRs, IC 443 and W44, W51C is a middle-aged SNR that is not expected to contain any longer the highest-energy cosmic rays it accelerated in its youth. All three of these objects require a broken power-law momentum spectrum of the protons. The break in the momentum spectrum is unconnected to the π^0 break in the γ-ray spectrum but is required to describe the high-energy part of the W51C γ-ray spectrum. The nature of the break in the parent particle population is unknown but since there is no energy-dependent morphology found in the *Fermi*-LAT energy range[5] two independent proton particle populations seem unlikely to

[5]There is strong evidence for an energy dependent morphology in the MAGIC data but the

explain the break. According to cosmic-ray diffusion models (Aharonian and Atoyan 1996; Gabici et al. 2009) the highest-energy cosmic rays start to escape from the middle-aged SNRs, but this scenario results in an exponential cut-off in the parent particle spectrum and not a break. Such an exponential cut-off is not sufficient to model the W51C data or that of the other two SNRs. Another possible explanation of a break in the proton spectrum is a modification of the shock acceleration due to the interaction with the surrounding MC, maybe by neutral ion damping as suggested in Malkov et al. (2011) for the case of W44. Another possibility might be that emission is generated through reaccelerating existing cosmic rays in SNR blast-wave triggered shocks in MCs (Uchiyama et al. 2010). In this scenario a break could be observed as an overlay of different acceleration zones in the MC that have varying densities (Uchiyama et al. 2010). In the case of W51C there is evidence for interaction between the SNR shell and adjacent MCs from multi-wavelength data. Also in W44 there is evidence for interaction with surrounding MCs (Uchiyama et al. 2012). On the other hand IC 443 is most likely not directly interacting with an MC and there is some diffusion required before the cosmic rays can interact with the MCs in the vicinity of the SNR shock and hence models for escaping cosmic rays were developed (Torres et al. 2010). The cause for the rather soft proton spectrum and the momentum break at few-to-hundreds of GeV$/c$ in these three SNRs can not be conclusively explained at present. The differences in the environments of these three SNRs might explain the differences in the break momentum and the spectral index change, but our knowledge of the exact environmental parameters is limited. Interestingly in all three cases an additional exponential cut-off in the γ-ray emission and in the parent particles is not detected. Therefore the highest-energy protons still accelerated by the SNR (or reaccelerated in the MCs) cannot be determined but must exceed about 30 TeV. Finding such high-energy protons in a relatively old SNR as W51C is surprising and future measurements with imaging Cherenkov telescopes, like the Cherenkov Telescope

---

break in the parent particle spectrum is already evident using only *Fermi*-LAT data.

Array, will reveal the acceleration capabilities of W51C. Also more detailed morphology studies of W51C will help to bring further insight to what part of the MC-SNR interaction leads to modifying the cosmic ray spectrum around the high-energy break and provide vital input to the development of theoretical models that will be able to explain the current data.

Acknowledgments

The *Fermi* LAT Collaboration acknowledges generous ongoing support from a number of agencies and institutes that have supported both the development and the operation of the LAT as well as scientific data analysis. These include the National Aeronautics and Space Administration and the Department of Energy in the United States, the Commissariat à l'Energie Atomique and the Centre National de la Recherche Scientifique / Institut National de Physique Nucléaire et de Physique des Particules in France, the Agenzia Spaziale Italiana and the Istituto Nazionale di Fisica Nucleare in Italy, the Ministry of Education, Culture, Sports, Science and Technology (MEXT), High Energy Accelerator Research Organization (KEK) and Japan Aerospace Exploration Agency (JAXA) in Japan, and the K. A. Wallenberg Foundation, the Swedish Research Council and the Swedish National Space Board in Sweden.

Additional support for science analysis during the operations phase is gratefully acknowledged from the Istituto Nazionale di Astrofisica in Italy and the Centre National d'Études Spatiales in France.

Facilities: *Fermi*-LAT

REFERENCES

Abdo, A. A., Ackermann, M., Ajello, M., et al.: 2009, ApJ, 706, L1

Acero, F. ,Ackermann, M., Ajello, M., et al.:2015 ApJS, 218, 23

Acero, F., Ackermann, M., Ajello, M., et al.: 2015, ApJ, submitted

Atwood, W. B., Abdo, A. A., Ackermann, M, et al.: 2009, ApJ, 697, 1071

Ackermann, M., Ajello, M., Albert, A., et al.: 2012, ApJS, 203, 4

Ackermann, M., Ajello, M., Allafort, et al.: 2013, Science, 339, 807

Ackermann, M., Albert, A., Atwood, W. B., et al.: 2014, ApJ, 793, 64

Aharonian, F. A. and Atoyan, A. M.: 1996, A&A, 309, 917

Aleksić, J., Alvarez, E. A., Antonelli, et al.: 2012, A&A, 541, A13

Baring, M. G., Ellison, D. C., Reynolds, S. P., Grenier, I. A., and Goret, P.: 1999, ApJ, 513, 311

Blumenthal, G. R. and Gould, R. J.: 1970, Reviews of Modern Physics, 42, 237

Casandjian, J.-M., Grenier, I., and for the Fermi Large Area Telescope Collaboration: 2009, ArXiv e-prints, astro-ph/0912.3478

Ceccarelli, C., Hily-Blant, P., Montmerle, T., Dubus, G., Gallant, Y., and Fiasson, A.: 2011, ApJ, 740, L4

Gabici, S., Aharonian, F. A., and Casanova, S.: 2009, MNRAS, 396, 1629

Green, A. J., Frail, D. A., Goss, W. M., and Otrupcek, R.: 1997, AJ, 114, 2058

Kamae, T., Karlsson, N., Mizuno, T., Abe, T., and Koi, T.: 2006, ApJ, 647, 692

Kerr, M.: 2011, PhD in Physics, University of Washington

Koo, B.-C., Lee, J.-J., and Seward, F. D.: 2002, AJ,123, 1629

Koo, B.-C., Lee, J.-J., Seward, F. D., and Moon, D.-S.: 2005, ApJ, 633, 946

Koo, B.-C. and Moon, D.-S.: 1997, ApJ, 475, 194

Lande, J., Ackermann, M., Allafort, A., et al.: 2012, ApJ, 756, 5

Malkov, M. A., Diamond, P. H., and Sagdeev, R. Z.: 2011, Nature Communications, 2, 194

Mattox, J. R., Bertsch, D. L., Chiang, J., et al.: 1996, ApJ, 461, 396

Mori, M.: 2009, Astroparticle Physics, 31, 341

Sato, M., Reid, M. J., Brunthaler, A., and Menten, K. M.: 2010, ApJ, 720, 1055

Vladimirov, A. E. et al. 2011, Computer Physics Communications, 182, 1156, 1008.3642

Su, M., Slatyer, T. R., and Finkbeiner, D. P.: 2010, ApJ, 724, 1044

Torres, D. F., Marrero, A. Y. R., and de Cea Del Pozo, E.: 2010, MNRAS, 408, 1257

Uchiyama, Y., Blandford, R. D., Funk, S., Tajima, H., and Tanaka, T.: 2010, ApJ, 723, L122

Uchiyama, Y., Funk, S., Katagiri, H., Katsuta, J., Lemoine-Goumard, M., Tajima, H., Tanaka, T., and Torres, D. F.: 2012, ApJ, 749, L35

This manuscript was prepared with the AAS LaTeX macros v5.2.